

Published in final edited form as:

*Conf Proc IEEE Eng Med Biol Soc.* 2009 ; 1: 630. doi:10.1109/IEMBS.2009.5334069.

## Finite Element Analysis of Electrical Impedance Myography in the Rat Hind Limb

**Mohammad A. Ahad and Seward B. Rutkove**

Beth Israel Deaconess Medical Center, Harvard Medical School, Boston, MA 02215 USA

Mohammad A. Ahad: mahad@bidmc.harvard.edu; Seward B. Rutkove:

### Abstract

Electrical impedance myography (EIM) is a form of muscle assessment based on the surface application of electrical current and measurement of the resulting voltages over a muscle group of interest. In order to better understand the effect of pathological change in muscle, EIM has recently been applied to the rat. In this study, a finite element model of EIM is presented for the rat hind limb which incorporates the detailed anatomy of the leg based on computerized tomographic imaging and conductivity and permittivity values obtained from the rat gastrocnemius muscle. In addition, the angular anisotropy of the biceps femoris muscle has been included. The model successfully predicts the recorded surface impedances measured with EIM.

### I. Introduction

Electrical Impedance Myography (EIM) is a recently developed, non-invasive technique to assess muscle status in healthy individuals and those with neuromuscular diseases. Unlike electromyography (EMG), which depends on the extraction of motor unit action potentials either by needle or surface electrodes, in EIM a low-intensity, high-frequency current is passed between two surface electrodes and the voltage is measured by another pair of electrodes residing in between the two current electrodes [1], [2]. Thus, the complex impedance can be measured for the muscle under investigation, including its resistance (R), reactance (X) and phase ( $\theta$ ), each of which can be used to help assess muscle condition.

Although EMG has proven itself of great value in neuromuscular diagnosis since the 1940s when the technique was first introduced into clinical practice, EMG parameters show substantial variability. This is true since needle EMG is very subject to sampling errors and generally relies upon qualitative ordinal grading scales. This technical limitation is most apparent when attempting to use EMG to follow the clinical status of a patient and response to treatment, for example. On the contrary, EIM variables appear highly reproducible. Our initial work on human [3], [4], [5] has already shown the potentiality of this new technique in a variety of neuromuscular diseases. In addition, EIM may be especially useful in children who usually cannot tolerate or cooperate with the multiple needle insertions required as part of a standard EMG study.

We are still in the relatively early stages of establishing EIM as a technique for neuromuscular disease detection and evaluation. Much of our EIM work thus far completed has been performed directly on human subjects. This has been advantageous in that we are able to study directly the diseases of interest but also because the relatively large size of human muscles makes the technique straightforward to employ. However, for obvious ethical reasons, we are

unable to determine how the surface EIM measurements relate to the actual underlying state of the muscle, since the latter would require actual tissue collection via biopsy. In fact, to fully interpret our EIM data in both normal and diseased muscle, it will be essential to analyze the actual histological and electrical properties of the muscle tissue itself. For this reason it became necessary to modify our human EIM techniques and apply them to animal models of neuromuscular disease. Thus, we have recently begun to apply EIM to the gastrocnemius-soleus complex of the rat hind-limb.

In this study, we describe the EIM technique in rats and develop a finite element model of EIM as applied to the rat hind limb, comparing actual surface EIM data with those derived from the finite element model. We also incorporate the effects of the biceps femoris muscle layer, which overlies the gastrocnemius-soleus muscle complex but whose fibers do not run parallel to it.

## II. Methods

### a. EIM data Collection

All studies were approved by the Institutional Animal Care and Use Committee at Beth Israel Deaconess Medical Center. Twelve Wistar rats of 16 weeks of age were obtained from Charles River, Wilmington, MA. Rats were anesthetized with isoflurane and the fur from the left hind leg was removed by clipping followed by the application of a depilatory cream. A small tattoo was then placed on the top of the skin approximately over the center of the gastrocnemius-soleus complex. This tattoo was used as a landmark to assist with accurate electrode positioning during subsequent EIM measurements. The rat was then placed on a heating pad and under a heat lamp, maintaining body limb temperature at approximately 37°C. The left hind limb was stretched at a 45° angle away from its body and maintained in this position by using a cloth retractor and tape.

Ambu Neuroline 700 surface adhesive Ag-AgCl electrodes (Product # 70010-K/C/12, AMBU Inc., Bethesda, Maryland) were used for EIM measurement. These electrodes are Ag-AgCl with a conductive adhesive gel. To facilitate our measurements on rats, these electrodes were resized to 2cm by 3.5mm by using a razor press customized for this purpose, which consistently produced electrodes of these exact dimensions. Each of these resized electrodes were placed upside-down in a line on a piece of adhesive tape with an inter-electrode distance of 0.75cm (center to center), such that the backing of the electrodes adhered to the tape. This approach helped assure a consistent inter-electrode distance, which would be very difficult to achieve if we were to place the electrodes individually on the muscle directly. The outer two electrodes served as the current electrodes and the inner two electrodes served as the voltage electrodes. The entire array was then placed on the shaved leg with the electrodes perpendicular to the long-axis of the limb, keeping the center of the electrode set aligned with the previously applied tattoo.

A multi-frequency lock-in amplifier, Model 7280 of Signal Recovery, Oak Ridge, TN coupled with a very low capacitance active probe (Model 1103 of Tektronix, Beaverton, OR) was used to measure the impedance of the muscle, as previously described [6]. Instrument-interfacing software was written in Visual Basic to display as well as store the recorded impedance data, including resistance and reactance in the frequency range of 500Hz to 2MHz, although for simplicity, in this study we report an analysis only incorporating the 50kHz data.

### b. FEM model

Whereas simple analytical models can be used for the analysis of regularly shaped bodies, numerical methods, such as the finite element method, are required for irregularly-shaped bodies including muscle. Two distinct current types contribute to the total current that flows

through muscle in EIM. One is a conductive or direct current that flows due to the movement of the charge particles and the other is the displacement current due to the changing electric field induced by the alternating current. Conductive current is defined as:

$$J_c = \sigma \cdot E \quad (1)$$

where  $\sigma$  is the conductivity of the tissue and  $E$  is the electric field.

The displacement current is given as:

$$J_d = \epsilon \frac{\partial E}{\partial t} \quad (2)$$

where  $\epsilon$  is the permittivity and  $\epsilon = \epsilon_0 \epsilon_r$  where  $\epsilon_0$  is permittivity of air ( $8.854 \times 10^{-12}$ ) and  $\epsilon_r$  is the relative permittivity. So the total current is given by:

$$J_{total} = J_c + J_d \quad (3)$$

In frequency domain, the total current is given by:

$$J_{total} = \sigma \cdot E + j\omega\epsilon_0\epsilon_r E \quad (4)$$

Since we are assessing the potential on the surface of the muscle, we must calculate the potential  $\phi$ , which is directly related to electric field as:

$$E = -\nabla\phi \quad (5)$$

In this simulation, the magnetic induction effects are negligible and the field is considered quasi static. Conservation of charge requires that:

$$\nabla \cdot J = 0 \quad (6)$$

Thus the equation that needs to be solved for the potential measurement is:

$$\begin{aligned} \nabla \cdot J_{total} &= \nabla \cdot (\sigma \cdot E + j\omega\epsilon_0\epsilon_r E) = 0 \\ &= \nabla \cdot [(\sigma + j\omega\epsilon_0\epsilon_r)\nabla\phi] = 0 \end{aligned} \quad (7)$$

A 1mA test current was supplied between the two current electrodes. The normal component of the electric current is assumed to be continuous between any two media. Also it is assumed that there is no current flow out of the boundary at the two ends of the model. This assumption is reasonable, as one side of the model ends at ankle and other side ends at knee, both consisting of mostly poorly conductive bone.

Our rat model consists of leg from ankle to knee joint which has a skin layer, a fat layer, the bicep femoris muscle, the gastrocnemius-soleus complex, and two bones (the fibula and the tibia). The shape of the leg was adopted from a computerized tomographic (CT) scan of the rat leg that we had been obtained while maintaining the rat in an identical position as when performing EIM. The fibers of the gastrocnemius-soleus complex muscle run roughly parallel

to the long axis of the limb, whereas fibers of biceps femoris run with a small angle  $\alpha$ . In addition, the biceps femoris tapers in thickness considerably distally. Thus angular anisotropy [7] was incorporated for this muscle layer. Comsol multiphysics software [8] (Comsol AB, Stockholm, Sweden) was used for this finite element analysis of the EIM in rat model. Electrode size and thickness were also modeled according to the actual size of the measuring electrodes. There were 60863 triangular 3D elements in the mesh.

### c. Measurement of dielectric properties

All rats were sacrificed after EIM measurements were completed to measure *in-vivo* dielectric constants of the gastrocnemius muscle. Dielectric properties were measured with a four electrode measurement technique. A plexiglass dielectric measuring cell was used which had a dimension of  $1\text{cm} \times 1\text{cm} \times 2\text{cm}$ . The top of the plexiglass cell was fitted with a removable plastic lid with four holes, each 2mm apart from each other and with the outermost holes also 2mm away from the edge of the cell. Freshly excised gastrocnemius muscle was cut into a 1 cm by 1cm piece by approximately 0.4 cm piece with a scalpel. The muscle was placed into the plexiglass cell in between two stainless steel current electrodes. These current electrodes were 1cm in width and 5 cm in length, and thus contacted entirely the two sides of the rectangular slab of muscle. Two disposable monopolar EMG needle electrodes of Viasys Healthcare (Ref# 902-DMG50) were used as two voltage-measuring electrodes. These two voltage electrodes were inserted through the holes of the plastic cover such that they just contacted the surface of the muscle. To insure consistent temperature, the entire cell was maintained at  $37^\circ\text{C}$  through the use of a heating pad surrounding the cell. Both longitudinal and transverse conductivities and permittivities were measured. Measurements were performed for needle electrodes distances of 4mm and 6mm using the system described above for the same range of frequencies. To minimize the effects of electrode resistance and reactance, we employed the technique described in [9].

Table 1 shows the measured longitudinal ( $\sigma_l$ ) and transverse ( $\sigma_t$ ) conductivities and longitudinal ( $\epsilon_l$ ) and transverse ( $\epsilon_t$ ) permittivities. These values are in good conformity with reported values in [10], [11]. For the purposes of employing the finite element method, isotropic conductivities and permittivities of skin, fat and bone were taken from [10], [12].

## III. Results

A complete finite element model is shown in Figure 1 with all layers labeled. Current density distribution is illustrated in Figure 2. Adult rats showed a surface resistance of  $73 \pm 4$  ohms (mean  $\pm$  SD) and reactance of  $23 \pm 2$  ohms. For a typical rat, the predicted values of resistance and reactance from the model are shown on Table 2 for varying  $\alpha$ , which is the angle between the fibers of biceps femoris muscle and the long-axis of the leg.

## IV. Discussion

These results show that employing the finite element method with actual electrical data obtained from excised muscle and a muscle shape based on CT imaging, we can obtain results in good agreement with our surface recorded EIM data. This analysis supports that modeling of EIM in rat holds the promise of being a valuable tool in interpreting the surface EIM data obtained as we move forward and apply EIM to the study of a variety neuromuscular diseases in rat models. Of importance, the rat EIM measurement methodology we have developed is relatively inexpensive to institute yet provides repeatable data with greater than 90% reproducibility [13].

There are several factors that will impact the outcome of the model results presented here. First, the conductivities and the permittivities measured need to be as accurate as possible. Achieving

this depends upon accurately measuring the muscle sample size, maintaining a consistent temperature, and performing the measurements as soon after sacrifice as possible, so as to avoid dehydration or degradation of the tissue. Second, the geometry of the leg incorporated in the model needs to be as accurate as possible. We attempted to model the geometry as if performing an actual EIM measurement by obtaining CT measurements with the leg in the same position as we perform EIM. Third, the actual anatomy of the internal structures of the leg (e.g. contribution of bone, skin and subcutaneous fat) needs to be reasonably accurate. These were incorporated also based on our CT and anatomical data. Finally the electrical properties of these other tissues also need to be accurately incorporated. Although we did not specifically measure the electrical properties of these tissues here, the values used were based on generally accepted values from the literature [10], [12].

It is of interest that the overlying biceps femoris muscle, despite being at a considerable angle to the gastrocnemius soleus complex, appeared to contribute minimally to the recorded data, and actually provided the most consistent reactance when no anisotropy was incorporated. In our model we used an average thickness of 2.25 mm, as compared to a thickness of 12 mm for the gastrocnemius-soleus complex, with the muscle tapering considerably toward its distal insertion point. However, it is possible that using a smaller dimension may have been more appropriate here.

We anticipate that in both myopathic and neurogenic diseases, the normal anatomy of the limb will be disrupted, and thus future finite element models will incorporate such variations. In addition, we suspect that actual electrical properties of the muscle itself will change and thus incorporating measurements of these values will also be important. Nonetheless, by employing finite element modeling in the rat hind limb, we hope to be able to better understand and interpret the marked changes in impedance measurements observed in human neuromuscular disease.

## Acknowledgments

This work was funded by grant R01055099 from the National Institutes of Health/National Institute of Neurological Diseases and Stroke

## References

1. Shiffman CA, Aaron R, Amoss V, Therrien J, Coomler K. Resistivity and phase in localized BIA. *Phys Med Biol* Oct;1999 44:2409–2429. [PubMed: 10533919]
2. Rutkove SB, Aaron R, Shiffman C. Localized bioimpedance analysis in the evaluation of neuromuscular disease. *Muscle Nerve* Mar;2002 25:390–397. [PubMed: 11870716]
3. Rutkove SB, Esper G, Lee K, Aaron R, Shiffman C. Electrical impedance myography in the detection of radiculopathy. *Muscle Nerve* Sep;2005 32:335–341. [PubMed: 15948202]
4. Rutkove SB, Zhang H, Schoenfeld DA, Raynor EM, Shefner JM, Cudkowicz ME, Chin AB, Aaron R, Shiffman CA. Electrical impedance myography to assess outcome in amyotrophic lateral sclerosis clinical trials. *Clin Neurophysiol* 2007;118:2413–2418. [PubMed: 17897874]
5. Tarulli A, Esper G, Lee K, Aaron R, Shiffman CA, Rutkove SB. Electrical impedance myography in the bedside assessment of inflammatory myopathy. *Neurology* Feb;2005 65:451–452. [PubMed: 16087913]
6. Kun S, Peura R. Effects of Sample Geometry and Electrode Configuration on Measured Electrical Resistivity of Skeletal Muscle. *IEEE trans on Biomedical Engineering* Feb;2000 47:163–169.
7. Esper G, Shiffman C, Aaron R, Lee K, Rutkove S. Assessing neuromuscular disease with multifrequency electrical impedance myography. *Muscle Nerve* Nov;2006 34:595–602. [PubMed: 16881067]
8. User's guide, Comsol Multiphysics. Comsol AB; Stockholm, Sweden: 2007.

9. Harty FX, Tollz RB, Bernerx NJ, Bennett NH. The low-frequency dielectric properties of octopus arm muscle measured *in vivo*. *Phys Med Biol* Oct;1996 41:2043–2052. [PubMed: 8912379]
10. Gabriel C, Gabriely S, Corthout E. The dielectric properties of biological tissues: I. Literature survey. *Phys Med Biol* Nov;1996 41:2231–2249. [PubMed: 8938024]
11. Stoy RD, Foster KR, Schwant HP. Dielectric properties of mammalian tissues from 0.1 to 100 MHz: a summary of recent data. *Phys Med Biol* 1982;27:501–513. [PubMed: 7089048]
12. Gabriel C. Dielectric properties of biological tissue: variation with age. *Bioelectromagnetics* 2005; (Supplement 7):S12–S18. [PubMed: 16142779]
13. Ahad MA, Rutkove SB. Electrical impedance myography at 50 kHz in the rat: technique, reproducibility, and the effects of sciatic injury and recovery. unpublished.

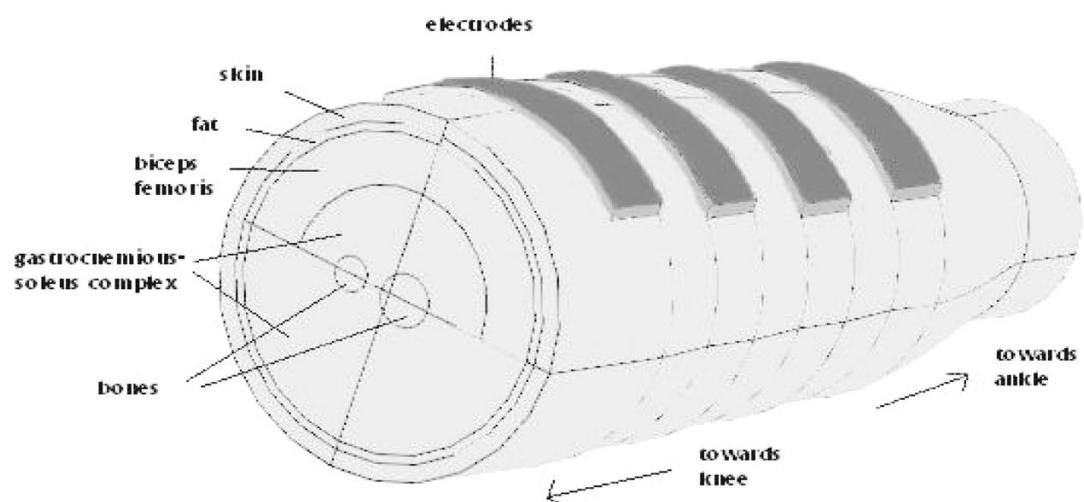


**Fig 1.**  
A complete FEM model of the rat hind leg.



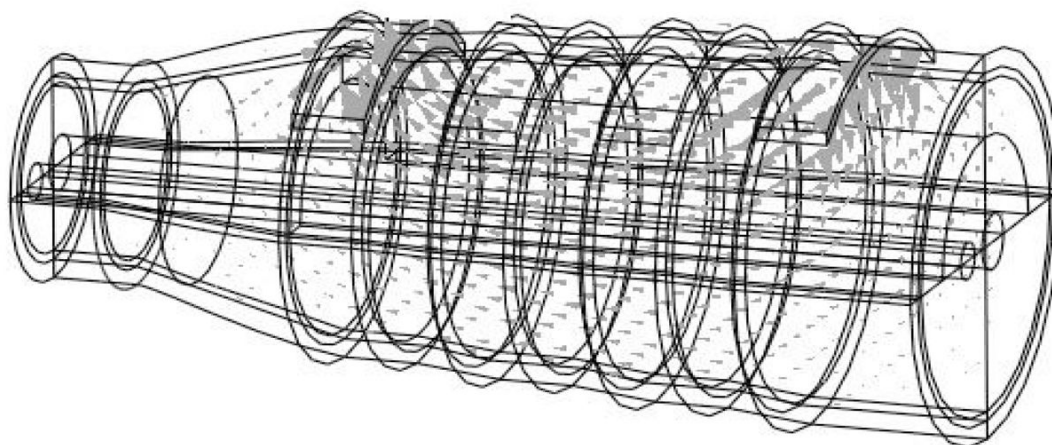


**Fig 2.**  
Current density distribution inside leg.



**TABLE I**

Measured conductivities and permittivities at 50kHz

$\sigma_l$ (S/m)	$\sigma_r$ (S/m)	$\epsilon_l$	$\epsilon_r$
0.36±0.04	0.17±0.02	41000±6500	35000±5000

**TABLE 2**

The impedance measured from the model

$\alpha$ (deg)	R (Ohms)	X (Ohms)
0	71	25
5	72	26
10	72	27
20	74	29